We would like to thank the referees for their detailed and constructive comments. We have revised the manuscript accordingly and our responses to the reviewers are below.


**Referee #1:  J.R. Barker**

**1. A quibble with the third-law analysis carried out in this paper is that it assumes that Keq is a pure exponential function, Keq = A exp(B/T), while theoretical calculations predict that Keq deviates slightly from a pure exponential. The approach taken in this paper differs from the third-law analysis carried out by the NASA/JPL Panel for Data Evaluation. The Panel evaluates every individual data point to determine the reaction enthalpy change at 0 K, ΔHr(0), extracted from the measured Keq(T) at each temperature and then determines the average. ΔHr(298) is then computed from the calculated reaction entropies and average ΔHr(0). From ΔHr(298), one can then obtain the standard enthalpy of formation, ΔHf(298), for ClOOCl. Although more laborious, the approach followed by the panel does not assume a pure exponential function and is thought to be more accurate. From the Panel's approach, the combined data set consisting of the new data from the present paper and the older data from Hume et al. (2015) gives ΔHr(298) = 130.1 kJ/mol, which is 0.2 kJ/mol higher than the result reported in the manuscript, based on the pure exponential function.**

We appreciate the approach described by the reviewer and the accuracy of this method for use in the NASA/JPL Data Panel Evaluation. However, to maintain consistency between our results and the method employed in prior papers (e.g., Hume et al. 2015), we have chosen to use the enthalpy values at 298 K for the calculations. Note that we now determine B from our unbinned data, and the calculated ΔHf(298) for ClOOCl is 130.0 kJ/mol, now in even better agreement with JPL-15 recommendation of 130.1 kJ/mol.

To facilitate alternate derivations of reaction enthalpies, all independent measurements are now reported in Table 1.


**2. In the abstract, it would be useful to state that the experimental errors are ±1 σ.**

The abstract now reads:
A third law fit of the equilibrium values determined from the experimental data provides the expression: Keq = 2.16×10−27e (8528 ± 25 K/T) cm3 molecule−1 (1σ  uncertainty).


**3. In addition to the binned values for Keq(T), which are reported in Table 1, all of the individual Keq measurements should be reported in Supporting Information.**

All independent measurements are now reported in Table 1.


**4. In Figures 4 and 6, the error bounds are functions of temperature. It would be useful to report the functional forms and parameters for the error bounds in Supporting Information.**

The error bounds of Figure 4 in the original manuscript (now Figure 5) are of the form: A exp (B±ε / T) from equation 2, where ε is the appropriate uncertainty interval. We now explicitly mention the ε value on page 7 line 9 of the revised manuscript.


**Referee #2:  M. von Hobe**

**1. Add more experimental information**
**I have little doubt that the authors have carefully checked the conditions of each experiment to ensure that thermal equilibrium between ClO and ClOOCl is actually established once the gas mixture passes into the absorption cell. Nevertheless, for the sake of transparency, it would be good to provide some actual numbers for flow rates and residence times in the different parts of the apparatus. Ideally, a complete set of experimental conditions (initial concentrations, pressure, $T_{ReactionCell}$, $T_{ColdT rap}$, $T_{EquilibriumCell}$) and selected results (maybe even some raw spectra) could be provided as an electronic supplement that goes beyond the summary given in Table 1.**

Table 1 has now been revised to include all of the experimental runs and not simply the binned data, and details on carrier gas flows and residence time have been added in section 2. We note that a critical element of the experimental design and operation was ensuring that ClO and ClOOCl were in equilibrium in the Absorption Cell when the measurements were made. As discussed in the manuscript, the kinetic model defined the experimental conditions (e.g., temperatures, pressures, concentrations) in which equilibrium would be achieved in the laboratory setup, and we operated experimentally across a range of conditions about the optimal starting conditions predicted by the model. In particular, we note that the same Keq values were obtained when increasing or decreasing residence times in the equilibrium and absorption cells, providing confidence that ClO and ClOOCl were indeed in equilibrium.


**2. Uncertainty assessment**
**I am not convinced that all potential sources of uncertainty are represented in the significantly reduced overall uncertainty presented in Figure 6. In particular, I'm thinking about the 17 % uncertainty in the ClOOCl reference cross sections that you mention on page 8, line 14. When I translate the uncertainty in the B parameter that accounts for this (given on page 8, line 17), I arrive at approximately +/- 40 % uncertainty in Keq, which is considerably larger than the uncertainty range given in Figure 6. There, it looks as if the blue uncertainty ranges only represent the statistical uncertainties in your experiment (i.e. the scatter between the individual white circles in that figure represented in the +/- 25 uncertainty in B given in Equation 3), and the statement about the trend to not explicitly include uncertainties from reference cross sections on page 6, line 21, seems to support that interpretation. In the work by Hume et al. (2015), there is a clear statement that the systemati uncertainties in cross sections to convert Kabs to Keq are much more important than their experimental standard deviations, and their error propagation calculations arrive at an upper uncertainty limit from this is 36 % on the experimental Keq, which appears to be a very realistic number. Note that the 17 % uncertainty in the ClOOCl cross section alone translates directly into a 17 % uncertainty in the ClOOCl concentration fitted to a particular spectrum, and in turn into a systematic 17 % uncertainty in Keq via your Equation 1. The two studies by Papanastasiou et al. (2009, currently the JPL recommended value and used in both, your study and Hume et al.) and Lien et al. (2009; 17 % higher) used different methods to measure absolute cross sections: Papanastasiou et al. infer the absolute value from the reaction stoichiometry and the experimental absorbance at isosbestic wavelength, while Lien et al. use a**
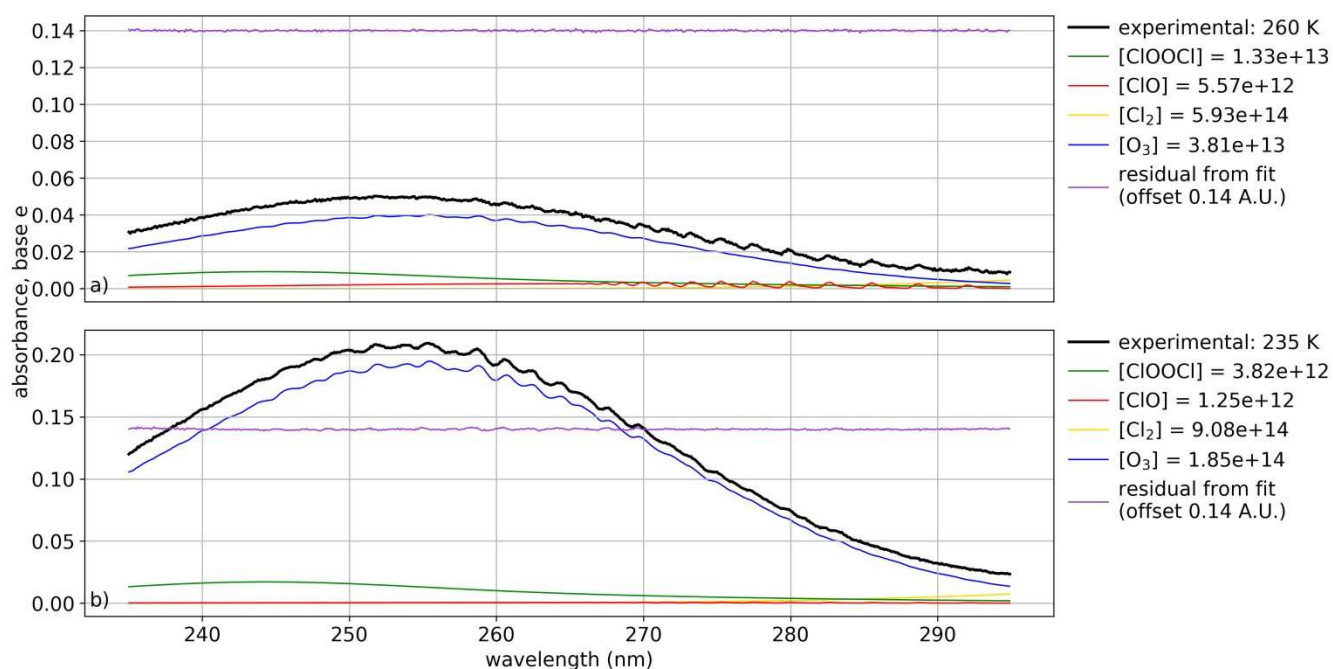
**known quantity of light to attenuate a molecular beam of ClOOCl. To date, no convincing evidence has been presented that proves either one of the results right or wrong. Therefore, the 17 % is not a statistical one or two sigma uncertainty, but a highly systematic one. As long as this is not resolved, it is therefore impossible to reduce the uncertainty in Keq below this value with any method relying on the ClOOCl cross sections. And because it is systematic, it really has to be added to the blue ranges representing the statistical uncertainties in your Figure 6, because if the peak ClOOCl absorption cross section was 17 % higher than the value you actually used in your calculations, all your points and the ones from Hume et al. would simultaneously down by 17 %. Of course, if the uncertainties in the ClOOCl cross sections were reduced in future studies, this would immediately also reduce the uncertainty in Keq, which I think would be a fair and valuable statement to make.**

It is true that the ClOOCl cross section directly impacts Keq, but to be clear, Hume et al. actually did not incorporate the ClOOCl cross section uncertainty into their reported Keq. Hume et al. used the larger uncertainty in the B parameter derived when considering the ClOOCl cross section uncertainty only when they assigned uncertainties to their enthalpy calculations. For consistency, we followed the same approach in our manuscript. Otherwise, we would be defining the uncertainty in Keq in a manner that is inconsistent not only with the recent Hume paper but all other published laboratory ClOOCl Keq papers that covered a range of temperatures, none of which include the uncertainty from the reference cross sections. We state on page 6 line 19 of the revised manuscript (page 6 line 21 of the original manuscript) that we are taking this approach, and on page 8 line 23 of the revised manuscript (page 8 line 17 of the original manuscript), we provide the larger uncertainty range in the B$parameter found when including the ClOOCl cross section uncertainty. We have also now added additional detail to Table 1 such that if the ClOOCl or ClO cross sections are revised in the future, our Keq values can be recalculated.

**Referee #3:  D. Toohey**
**1. Please show an enlargement of residual spectra (e.g., as in Figure 2) with examples calculated at the 1-sigma ranges of the uncertainties. This is especially important for the results at lowest temperatures where ClO absorbances are smallest relative to total absorbance due to the [ClO]-squared nature of Keq.**

The figure requested is shown below for two independent experiments in which the calculated $K_{eq}$ approximates the 1-sigma uncertainties. Note that the Y axes are different between the two panels. Again, as in Figure 2 of the manuscript, OClO and Cl2O3 are included in the fit, but excluded from the visualization as their formation is suppressed by the operation of the reaction cell at 200 K and would appear as flat lines at the 0 A.U. line of each panel.

**The figure requested is shown below for two independent experiments in which the calculated $K_{eq}$ approximates the 1-sigma uncertainties. Note that the Y axes are different between the two panels. Again, as in Figure 2 of the manuscript, OClO and Cl2O3 are included in the fit, but excluded from the visualization as their formation is suppressed by the operation of the reaction cell at 200 K and would appear as flat lines at the 0 A.U. line of each panel.**

In this case the difference is minimal, but we agree that it is more appropriate to fit the Keq values from individual replicates rather than the binned data. A third law fit of all independent measurements produces a B parameter value of 8528 K, which represents a change of 0.059% from the value of 8533 K reported in the original manuscript. We have revised the manuscript throughout to reflect this value.

A new Figure 3 now appears in the manuscript and is replicated below. In this figure, the independent experimental results are indicated as small orange circles and are used to determine the black fit line. Note that the density of orange points is obscured for some temperatures where the scatter is small, and thus the updated Table 1 should be referenced.
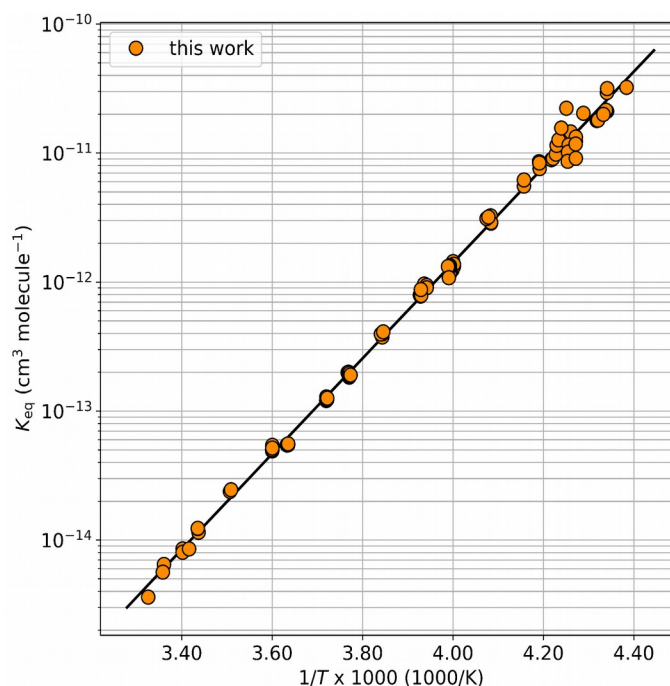
**3. Because of the strong dependence of Keq on temperature, a more detailed description of temperature variations and accuracy is essential. Please show (or describe) how temperature varies axially and radially within the measurement cell during a given replicate. Also, it would be useful to know how much temperature varies with time over the course of a particular replicate. I am a little concerned that a single-point measurement of temperature in the center of a measurement cell may not be adequate for a quantitative assessment of uncertainties (e.g., note that a 1.0 degree variation in temperature translates into a 15% variance in Keq). Presumably the uniformity of temperature has been carefully measured and documented at various temperatures. If so, presentation of such evidence will greatly strengthen the case that this new measurement can be used to reduce uncertainties in the JPL assessment.**

As shown in Figure 1 of the original manuscript, the temperature measurements were conducted at several key points (including immediately prior to the entrance of the gas mixture to the absorption cell and at the halfway point of the absorption cell). For all results reported in this work, the temperature difference between these points was less than 1 K. Radial measurements of the temperature gradient were also performed. Temperature differences of less than 0.5 K were observed between the wall region and the center of flow. We note that, to optimize lamp signal (i.e., to avoid clipping the light), the thermistor junction in the absorption cell was maintained at an intermediate position between the wall and the center of flow for all experimental results reported in this work.

Absorbance and equilibrium cell temperatures can be maintained at a near-constant temperature for an indefinite period of time and are well-insulated from any interference from the surrounding environment.  The insulating material used here, cryogel-Z, is an extremely high-quality insulating material. There was never any condensation of water on the experiment, even when operating at 203 K (the lowest attainable temperature of the experiment) for several hours.  Gas temperature was observed to remain static (variation within the noise levels of the thermistor ADC) over the course of a single sample acquisition (3 minutes time).

**4. I appreciate the rationale for co-varying pressure and temperature; however, given the possibility of systematic biases due to pressure (e.g. secondary reactions), it would be useful to know if any detailed measurements with varying pressure were carried out for a fixed temperature. On Page 6, starting on Line 10, the authors state "The precision of repeated measurements conducted at the same temperature but varied flow rates and pressures did not statistically deviate from the precision from temperature dependence alone." Over what range (or percentage) were flow rates and pressures varied for a fixed temperature? Or does this refer to unintended variations that may have occurred over the course of a particular replicate?**

Experiments were performed at a selection of pressures in order to verify asymptotic equilibrium behavior at a fixed temperature. It was typical to scan pressures by +/- 20% of the target pressure when evaluating conditions prescribed by the kinetic model. Pressure and flow rates were maintained at a constant value during sample acquisition.

**5. The authors need to show a more detailed error analysis that traces the various sources of error (e.g., from spectral fitting, temperature, and errors in rate parameters for interfering secondary reactions, if relevant). They should also include an assessment of potential systematic errors (such as those described above). They could expand Table 1 to include these errors. I am not sure that the standard deviation values listed in Table 1 are uniformly illustrative - for example, there is no way that a 0.3% standard deviation from two independent measurements at 285.1 K is representative of the true precision when the standard deviation is 10% for the 8 replicates at 253.3 K.**

Page 6 of the original manuscript contains a detailed assessment of error from spectral fitting, temperature-dependence, and other obvious potential systematic errors. As for secondary reactions such as the formation of OClO and higher oxides of chlorine, these are highly suppressed in our system due to the operation of the reaction cell at cold temperatures. The Figure 2 caption states that OClO and $Cl_2O_3$ concentrations were small (and even if present, they would not compromise the experiment, because they are included in the spectral fits).  We also point out that we essentially quench the Cl + ClOOCl reaction pathway by operating the experiment with an excess of ozone.

We have revised the method by which we calculate $K_{eq}$, now evaluating each independent measurement separately in an ordinary least squares fit. Because of this, metrics required for the reproduction of the weighted-least squares fit of the binned data, such as standard deviations of similar-temperature replicates, have been removed from Table 1.

**Minor comments**
**6. Abstract/conclusions. The authors should report the value of Keq over the temperature range 230 to 299 K, reflecting the range over which they have calculated their experimental averages. Alternatively, if they want to claim significance for a measurement at 288 K then they should report a value that is measured over the range 285.5 to 290.5 K (assuming a similar 5 degree average).**

We now calculate Keq using every independent replicate, spanning the temperature range of 228 – 301 K.

**7. Page 2, line 28. Please elaborate on ". . .optimization of target chemistry." What, specifically, was optimized?**

The various flow sections shown in Figure 1 are operated at the optimal conditions for achieving thermal equilibrium. This sentence is simply an introduction to the flow section descriptions that follow.


**8. Page 2, lines 30-31. Discuss whether or not you expect discharge of oxygen to produce O2(singlet delta), and if so, how you might expect reactions of this specie to impact your results.**

$N_2/O_2/O_3$ addition is performed downstream of the microwave discharge, which maintained a constant salmon color when chlorine was not injected and a constant deep purple color when chlorine was injected. The color of the discharge did not change when $O_2/O_3$ flows were turned on. When pressure was scanned above 533 mbar, the discharge was observed to turn white, indicating backflow of nitrogen from the injector port. All reported experiments were conducted below 333 mbar.

The exact placement of the microwave cavity relative to the $O_3$ addition port varied for some experiments, as did the size of the discharge depending on flow conditions, but during operating conditions as reported in this work (100 – 333 mbar), we observed no interfering absorbers in the UV spectra (e.g., residual traces were homoskedastic). We observed no evidence of interference from excited oxygen or nitrogen species produced in the microwave discharge.


**9. Page 3, line 30. Please list your carrier gas flow rates and residence times in each of the cells.**

Flow rates for the carrier gases ranged between ~1.0 – 1.8 L/min and residence times in the absorption cell ranged between ~1 – 11 seconds, depending on pressure and temperature. These values have been added to the manuscript on page 3 line 30 and page 4 line 2.


**10. Page 7, lines 31-33. It might be helpful to include a representative 1 sigma uncertainty bar on the results from the February 3, 2000, SOLVE/THESEO ER-2 flight in Figure 5. Please note whether "measurement uncertainties" for those data points refer to uncertainties (or variability) in measured concentrations of ClO and ClOOCl, uncertainties (or variability) of measured temperature, or both. This could also be illustrated with the use of vertical (for concentrations) and horizontal (for temperature) error bars.**

Including the 2-sigma uncertainties, all of the SOLVE/THESEO data points overlap the 2-sigma uncertainty range of our fit. This fact is now stated in the manuscript on page 8 lines 3 – 5.


**11. Page 9, line 8. You might elaborate on how, specifically, the uncertainties in JPL recommended Keq can be reduced. Should results of previous experiments be discounted by the JPL panel? Or should results of various experiments over the years be averaged and weighted according to errors reported at the time?**

The current uncertainty envelope is derived from the minimum uncertainty required to envelop the independent results of Cox and Hayman (1988), Nickolaisen et al. (1994), and Hume et al. (2015). Our results exhibit significantly less scatter than the two earlier studies. Though we do not presume to tell the JPL panel how to evaluate the uncertainty of the ClO/ClOOCl equilibrium constant, a similar approach to the one conducted to determine prescribed uncertainty for the 2015 data evaluation using our work instead of the older studies would produce a significantly smaller uncertainty.

**Referee #4:  Anonymous**

**The microwave discharge that generates atomic chlorine will also be a strong source of VUV radiation due to the strong Cl resonance lines. Since the ozone is introduced only 2.5 cm downstream, one would expect significant photolysis of the ozone, generating C1 O(1D), O(3P), O2(a1delta), etc. Also the discharge that generates ozone will also form copious amounts of the singlet states of O2. Does the chemical modeling of this system show that none of these reactive species are causing trouble downstream?**

There was no evidence that secondary reactions interfered with our measurements. O3 was transported ~3 m subsequent to generation prior to injection into the experiment. O2(singlet delta) would certainly be quenched prior to injection over this length scale. We observed no evidence of interfering species in the absorbance spectra after fitting for known species (e.g., residual was homoskedastic).

During initial setup and calibration of the apparatus, experiments were performed in which the microwave cavity was placed at varying distances from the ozone injection port and ClO absorbances were quantified. The selected position of the cavity, ~2.5 cm upstream of the ozone injector, was found to be the optimal position for production of ClO (competing with the recombination of Cl). Please our response to Referee #3 for additional details on this topic.

**Typical gas flow rates or the velocities of the flows at the different pressures should be given**

We have revised page 3 line 30 and page 4 line 2 of the manuscript to provide this information.

**Page 4, line 5: What is the resolution (FWHM) for this slit width?**

The grating and slit width combination produce a resolution of ~0.3 nm. Page 4, line 5 of the revised manuscript now includes this information.

**Page 4, line 10: What are "dark spectra" and how are they used in subsequent spectra?**

Prior to any day of experiments, a spectrum is collected in which the UV lamp is off. This spectrum is subsequently subtracted from all subsequent spectra to provide a correction for dark current in the photodetector.

**The two runs shown in Fig. 2 can be used to calculate two equilibrium constants: for 230K, K = 1.84E(-11) which is 34% lower than Equation 3 predicts; for 300K, K = 6.52E(-15) which is 34% higher than Eq.3. Are these typical deviations?**

The spectra presented in Figure 2 were selected because they both featured very similar concentrations of O3, allowing for comparison of the fit residual on the same scale. While these spectra are both members of the experimental ensemble reported, they are far from the best examples we could have chosen here to produce a Keq in close agreement with the mean reported value. A full list of independent experiments is now presented in Table 1.

**The treatment of the experimental data by "binning" is not the best use of the experimental data. If I understand this manuscript correctly, all values of K measured within a 5 K range of temperatures are averaged (average of K, or ln(K)?) and then listed in Table 1 along with the averaged temperature (average T or 1/T?). For example, if measurements were done at 250 and 255 K, one should get, according to Equation 3, K(250) = 1.438E(-12) and K(255) = 7.364E(-13). The average of ln(K) of these two K's gives -27.602 or K(ave) = 1.029E(-12), which is close to the value predicted by Eq. 3 for T = 252.5 K. But then using the deviations of these two values of K from the average K to get an estimate of the standard deviation of the measurements is not valid. There is no information about the random measurement errors in these two numbers. They are different because they were measured at two different temperatures. Supposed one has only two measurements in one bin that were are different temperatures but, due to random errors, gave almost the same value for K. The calculated "standard deviation" would now be very small and the weighting factor very large. That is not right. The numbers in the last column in Table 1 should be eliminated. It would be better to do the least squares fitting using all 114 experimental measurements with equal weighting. Then the deviations of the experimental K values from the least squares fit would give information about the precision of the measurements.**

In this case the difference is minimal, but we agree that it is more appropriate to fit the Keq values from individual replicates rather than the binned data. A third-law fit of all independent measurements produces a B parameter value of 8528 K, which represents a change of 0.059% from the value of 8533 K reported in the original manuscript. We have revised the manuscript throughout to reflect this value.

**A plot of these 114 deviations vs. 1/T would be useful. As mentioned, this will probably show increasing deviations at both the upper and lower limits of temperature.**

The reviewer is correct that there are increasing deviations at the upper and lower limits of temperature. A new Figure 3 of all independent results is now included in the manuscript.

**Certainly the experimental values of the 114 measurements should be preserved, either in a table in the manuscript or as supplemental material.**

These independent measurements are now included in Table 1.

# UV spectroscopic determination of the chlorine monoxide (ClO) / chlorine peroxide (ClOOCl) thermal equilibrium constant

J. Eric Klobas[1] and David M. Wilmouth[1]

[1]Harvard John A. Paulson School of Engineering and Applied Sciences and Department of Chemistry and Chemical Biology, Harvard University, Cambridge, MA 02138, USA

**Correspondence:** J. Eric Klobas (klobas@huarp.harvard.edu)

**Abstract.** The thermal equilibrium constant between the chlorine monoxide radical (ClO) and its dimer, chlorine peroxide (ClOOCl), was determined as a function of temperature between $228 - 301$ K in a discharge flow apparatus using broadband UV absorption spectroscopy. A third law fit of the equilibrium values determined from the experimental data provides the expression: $\cancel{K_{eq} = 2.16 \times 10^{-27} e^{(8533 \pm 25 \text{ K}/T)}}$ $K_{eq} = 2.16 \times 10^{-27} e^{(8528 \pm 25 \text{ K}/T)}$ cm$^3$ molecule$^{-1}$ (1$\sigma$ uncertainty). A second law analysis of the data deviates minimally: $\cancel{K_{eq} = (2.06 \pm 1.27) \times 10^{-27} e^{(8546 \pm 123 \text{ K}/T)} \text{ cm}^3 \text{ molecule}^{-1}}$ $K_{eq} = (2.14 \pm 1.14) \times 10^{-27} e^{(8530}$ From the slope of the van't Hoff plot in the third law analysis, the enthalpy of formation for ClOOCl is calculated, $\Delta H_f^\circ (298 \text{ K})$ = $\cancel{129.9}$ $130.0 \pm 0.6$ kJ mol$^{-1}$. The equilibrium constant results from this study suggest that the uncertainties in $K_{eq}$ recommended in the most recent (year 2015) NASA JPL Data Evaluation can be significantly reduced.

## 1 Introduction

Halogen-mediated catalytic processing of ozone accounts for the overwhelming majority of lower stratospheric ozone-loss processes in polar winter and spring (e.g., WMO, 2014; Wilmouth et al., 2018). Approximately half of this loss (Wohltmann et al., 2017) is resultant from the ClO dimer cycle (Molina and Molina, 1987), which occurs as a result of the highly perturbed physicochemical conditions of the polar vortices:

$$\text{ClO} + \text{ClO} + \text{M} \rightleftharpoons \text{ClOOCl} + \text{M} \tag{R1}$$

$$\text{ClOOCl} + h\nu \rightarrow \text{ClOO} + \text{Cl} \tag{R2}$$

$$\text{ClOO} + \text{M} \rightarrow \text{Cl} + \text{O}_2 + \text{M} \tag{R3}$$

$$2\,(\text{Cl} + \text{O}_3 \rightarrow \text{ClO} + \text{O}_2) \tag{R4}$$

net: $2O_3 \rightarrow 3O_2$ (R5)
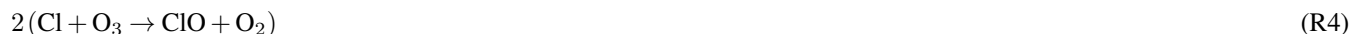
Within this cycle, the equilibrium governing the partitioning of ClO and ClOOCl in reaction (R1) is defined as:

$$K_{eq} = \frac{[\text{ClOOCl}]}{[\text{ClO}]^2} \tag{1}$$

This thermal equilibrium is a key parameter that determines the nighttime partitioning of active chlorine in the winter-spring polar vortex. The value of $K_{eq}$ can also tune the efficiency of chlorine-mediated ozone destruction, particularly the radial extent of ozone loss within the warmer Arctic polar vortex. For example, Canty et al. (2016) quantified how small variations in $K_{eq}$ can modulate significant changes in the temperature at which photolysis of ClOOCl and thermal decomposition of ClOOCl occur at equal rates.

Although the partitioning between ClO and ClOOCl is highly important, relatively few laboratory measurements of $K_{eq}$ have been made, and there is significant disagreement between reported values. Accordingly, the uncertainty in $K_{eq}$ was large (e.g., ~75% at 200 K) as of the 2011 JPL compendium recommendation (Sander et al., 2011). The most recent 2015 JPL-recommended value of $K_{eq}$ was revised on the basis of a 2015 study by Hume et al. (2015), but the recommended uncertainties are still substantial—exceeding 50% at 200 K (Burkholder et al., 2015).

The preponderance of laboratory data from previous determinations of $K_{eq}$ was obtained at temperatures significantly warmer than the polar stratosphere ($T > 250$ K). Error in the extrapolation of these warm temperature data has often been cited to explain the lack of correspondence between values of $K_{eq}$ determined in the laboratory and those calculated from stratospheric observations (Avallone and Toohey, 2001; Stimpfle et al., 2004; von Hobe et al., 2005; Santee et al., 2010). The more recent results of Hume et al. (2015) are unique in that they were obtained at temperatures colder than other laboratory studies (206 K < $T$ < 250 K), but their experimental method was compromised by secondary bimolecular reactions at warmer temperatures. In the present study, our spectroscopic data bridge the warmer temperatures where most laboratory determinations of $K_{eq}$ have been made to the colder temperature work of Hume et al. (2015), covering a broader temperature range than any previous study. The thermal equilibrium constant between ClO and ClOOCl was measured as a function of temperature (228 K < $T$ < 301 K) by UV spectroscopy and is evaluated here in relation to prior determinations, observations, and compendial recommendations.

## 2 Experimental

All experiments were conducted in a discharge flow apparatus, as shown in Figure 1. Independently programmable thermal zones allow for the optimization of target chemistry as a function of flow velocity, temperature, and pressure. ClO is synthesized via the reaction of Cl atoms with $O_3$ (reaction R4). Cl is produced from a 1% $Cl_2$/He gas mixture, diluted further with UHP He and directed through a 45 W, 2.45 GHz microwave discharge. $O_3$ is produced via electric discharge of a 10% $O_2$/Ar source mixture and subsequently introduced 2.5 cm after the microwave cavity. Once formed, ClO readily dimerizes to form ClOOCl (reaction R1), particularly at higher concentrations and colder temperatures.

To facilitate dimerization of ClO, the gas mixture is cooled in a 20-cm long jacketed quartz cell immediately subsequent to the microwave discharge. This reaction cell (Figure 1) has an inner diameter of 1 cm and can be maintained at a temperature between 198 – 305 K via circulating chilled methanol (NESLAB Endocal ULT-80). The operation of this cell at cold temperatures additionally suppresses undesired chemistry, preventing the synthesis of side products such as OClO per reaction R6, and subsequently $Cl_2O_3$ per reaction R7.

$$ClO + ClO \rightarrow OClO + Cl \tag{R6}$$

$$ClO + OClO + M \rightarrow Cl_2O_3 + M \tag{R7}$$

Following the reaction cell, the gas stream then passes through the cold trap zone, which is maintained at temperatures between 100 K and room temperature depending on the experiment. Cooling is accomplished by flowing $N_2$ gas through a copper coil immersed in liquid $N_2$ and then through an 18-cm long insulated aluminum jacket surrounding the 1-cm inner diameter quartz flow tube. Type K thermocouples (alumel/chromel) are affixed at three positions on the outside of the flow tube, opposite the cryogenic gas ports. These thermocouples are further insulated to ensure the recorded voltages correspond to the temperature of the quartz tube and not the temperature of the cryogenic gas. The coupling between the cold trap and the equilibrium cell is actually linear but is presented as a right angle in Figure 1̶1 for graphical purposes.

The next section of the flow system in Figure 1, labeled equilibrium cell, is a jacketed 50-cm quartz tube of 1-cm inner diameter. This section is where the gases reach equilibrium prior to measurement in the absorption cell. The equilibrium cell and the absorption cell share a coupled circulating chilled methanol bath (NESLAB ULT-80) ensuring that the two cells are maintained at the same temperature. The equilibrium cell is isolated from the environment with two 10-mm blankets of aerogel insulation (Cryogel Z). Additionally, a flow of cryogenic $N_2$ passes through an insulated aluminum jacket surrounding the union between the equilibrium cell and the absorption cell. This $N_2$ is chilled by passing through a copper coil immersed in the reservoir of the circulating chiller servicing the reaction cell, and the flow is modulated to provide constant temperature as the gas mixture transits from the equilibrium cell to the detection axis. A 100 Ω thermistor is inserted into the gas stream at this location to verify the temperature.

Finally, the gas mixture enters the absorption cell, a 91.44-cm jacketed quartz tube with an inner diameter of 2.54 cm. This detection axis is oriented at a right angle to the equilibrium cell and is terminated with two quartz windows. A 100 Ω thermistor is positioned at the halfway point. Cryogenic circulating methanol provides for temperature control between 228 – 301 K. Two 10-mm blankets of aerogel insulation (Cryogel Z) provide thermal isolation from the environment. An exterior dry $N_2$ purge is employed to prevent window condensation.

The discharge reactor is operated at pressures between 100 – 333 mbar. Pressure is monitored with Baratron capacitance manometers. Carrier gas flow rates, ~1.0 – 1.8 L min$^{-1}$ depending on the experimental conditions, are metered via MKS mass flow controllers. $Cl_2$ flow rates are controlled via a needle valve, while $O_3$ addition is modulated using micrometer flow

control valves. Total system pressure and velocity are tuned using an integral bonnet needle valve. ~~Residence times within the~~ ~~absorption cell range between ~1 – 11 seconds, depending on gas flow rates, system temperature, and pressure.~~ A quarter-turn
5   plug valve provides a bypass of the integral bonnet needle valve such that rapid pump down of the reactor and reignition of the plasma can be performed without disturbing pressure calibration during the course of experiments.

    Data were acquired using a fiber-coupled Ocean Optics USB4000 UV-Vis spectrometer (~~10-$\mu$m slit width, 200–400 nm~~ ~~grating~~ ~0.3 nm resolution) illuminated by a Hamamatsu L2D2 deuterium lamp. The need to correlate Baratron, thermocouple, and thermistor sensor readings with each UV spectrum required the in-house development of custom software. Drivers and
10   libraries to operate the spectrometer and simultaneously interrogate analog sensors were written in Python 2.7 and, in combination with the Python-Seabreeze library, provided scriptable, automated control of nearly all aspects of the data acquisition system.

    The deuterium lamp was allowed to warm up for at least one hour prior to data collection activity to reduce small variations in lamp output on experimental timescales. Dark spectra were acquired prior to any experiments on a daily basis. Background
15   spectra were obtained with the microwave plasma extinguished and all gas flows of species that absorb in the region of 200 – 295 nm (e.g. $O_3$, $Cl_2$) off. For consistency, sample spectra were obtained exactly 100 seconds after the background spectra against which they were referenced. Each saved spectrum consists of the co-addition of 597 individual scans, the number of scans that could be obtained in exactly 3 minutes of acquisition time.

    To aid in the selection of experimental conditions, a simulation of the discharge-flow reactor was constructed. A numerical
20   integrator for chemical kinetics (written in Python 2.7 with NumPy and SciPy) for 18 chemical species and 45 relevant chemical reactions was informed by JPL Data Evaluation 15-10 kinetic rate constants (Burkholder et al., 2015) and coupled into a physical model of gas flows as a function of reactor geometry, temperature, and pressure. Temperature and pressure ranges were scanned to determine optimal conditions to ensure ClO-ClOOCl equilibrium within the real-world experiment. Because parameterized simulations carry inherent uncertainty, experimental conditions were selected at several pressures along the
25   equilibrium asymptote ($K_{eq}$ vs $P$), and real-world experiments were performed at pressures above and below the identified value in order to confirm asymptotic equilibrium behavior. The kinetic model was only used to inform conditions for the experimental setup, but no results from the model were used in the determination of the reported equilibrium constants.

## 3   Results and Discussion

More than 136,000 background and sample spectra were obtained between the temperatures of 228 – 301 K at pressures rang-
30   ing between 100 – 333 mbar. Typical initial concentrations spanned $2\times10^{13} - 4\times10^{14}$ molecules cm$^{-3}$ for $O_3$ and $1\times10^{14} - 4\times10^{15}$ molecules cm$^{-3}$ for $Cl_2$. Active chlorine (ClO$_x$) concentrations were typically $1 \times 10^{13} - 1 \times 10^{14}$ molecules cm$^{-3}$ with the microwave discharge on. These values were tuned according to the initial conditions prescribed by the model simulations, as described above. For example, as the target temperature of the experiment decreased, the system was operated at incrementally higher pressures to allow more time for equilibrium to be achieved. Higher temperature samples reached equi-

librium more readily, so gas velocity was increased to limit the impact of enhanced rates of secondary chemistry on observed $K_{eq}$ values.

5     Multicomponent spectral curve fitting software packages were programmed in Python 2.7/LmFit (Newville et al., 2016) for the deconvolution of the UV absorption spectra of $O_3$, $Cl_2$, ClO, ClOOCl, OClO, and $Cl_2O_3$. Reference cross sections were utilized as follows: For $O_3$ and OClO, pure sample spectra were acquired and scaled to match the 2015 JPL-recommended cross sections of Molina and Molina (1986) and Kromminga et al. (2003), respectively. ClOOCl and $Cl_2O_3$ cross sections were obtained directly from the 2015 JPL data evaluation (Burkholder et al., 2015). Temperature-dependent cross sections of

10  $Cl_2$ were obtained from Marić et al. (1993) and validated to match observed $Cl_2$ spectra along the experimental temperature range. Synthetic temperature-dependent cross sections from Marić and Burrows (1999) were used for ClO due to the broad temperature range over which the data are available.

    The cross sections from Marić and Burrows (1999) were found to provide an excellent fit of experimentally obtained ClO at all relevant temperatures in this study and were validated against available laboratory-determined ClO cross sections from

15  the literature. Our experimental spectra at 263 K fit using both the synthetic ClO cross sections of Marić and Burrows (1999) and the reported experimental cross sections of Trolier et al. (1990) at 263 K result in concentrations of ClO that differ by only 1.6%. Similarly, experimental samples at 300 K from this study fit to the room temperature, laboratory ClO cross sections of Simon et al. (1990) and Sander and Friedl (1988) have excellent correspondence with the synthetic cross sections of Marić and Burrows (1999): 1.9% deviation in ClO concentration in comparison with Simon et al. (1990) and 2.7% deviation in comparison

20  with Sander and Friedl (1988). The resolution of our experimental spectra was degraded to match the lower resolution data of Trolier et al. (1990) for this comparison, while the cross sections of Sander and Friedl (1988) and Simon et al. (1990), which were published at higher resolution than provided by our spectrometer, were degraded to our spectral resolution.

    For all reported experiments, spectra were fit between 235 – 295 nm in order to capture the peak absorbances of both ClO and ClOOCl. Figure 2 provides example fits at (a) 230 K and (b) 300 K. In both cases, the residual (offset 0.14 A.U. for clarity)

25  is observed to be flat and minimally structured, and this holds true for all spectral fits reported in this work. In those places where the residual is structured, the structure is primarily resultant from mismatch in instrument function between reference and experimental spectrometers. Once the ClO and ClOOCl concentrations are determined from the spectral fit, the value of $K_{eq}$ at the relevant temperature is calculated per equation (1).

~~For reporting and analysis purposes, data points were collected and binned in 5 K intervals.~~ A total of 87 independent

30  experimental observations of $K_{eq}$ ~~values were then obtained and reported as the average $K_{eq}$ at the average temperature within the binning interval. These values~~ were acquired. The results are plotted in Figure 3 as a function of inverse temperature and are enumerated in Table 1. Data were considered independent when experimental conditions were modified between sample acquisitions (e.g., change in initial gas concentrations, pressure, temperature, carrier gas flow rates, or microwave discharge power). Data points that were not independent were reduced to a single independent data point by coaddition. Samples at colder temperatures were subjected to more repeated evaluations to improve accuracy under the low ClO conditions.

    The ~~$\log_{10}$ of these $K_{eq}$ values is plotted a function of inverse temperature in Figure 3 (purple circles). Equilibrium constants determined from other laboratory studies are indicated on the same figure for comparison. Notably, the $K_{eq}$ values reported in~~

~~this work are typically smaller than prior evaluations of $K_{eq}$ at warmer temperatures but match well with the colder temperature~~

5 ~~observations of Hume et al. (2015) for those data points with overlap (228 –250 K).~~

~~The~~ temperature dependence of $K_{eq}$ can be related as an Arrhenius expression, per equation (2), with free parameters $A$ and $B$.

$$K_{eq} = Ae^{(B/T)} \tag{2}$$

In a third law fit, the prefactor $A$ is fixed to a prescribed value. For this work, we employ the JPL Data Evaluation recom-

10 mended $A$ parameter value of $2.16 \times 10^{-27}$ cm$^3$ molecule$^{-1}$, which is the most recent literature evaluation of this constant (Burkholder et al., 2015). A third law fit of our $K_{eq}$ data yields a $B$ parameter value of ~~8533~~ 8528 K. This result was obtained by ~~nonlinear weighted~~ an ordinary least-squares ~~with a weighting factor of $N/S^2_{K_{eq}}$, in which $N$ is the number of replicate measurements at each temperature bin and $S_{K_{eq}}$ is the standard deviation among those replicate measurements~~ fit of the independent measurements of $K_{eq}$ (Table 1). The fit is shown in Figure 3 as the black ~~line and matches well with the results~~

15 ~~of Hume et al. (2015) when extrapolated to 200 K~~ trace. Error from the fitting process was quantified via bootstrapping with 2000 resamplings of the binned $K_{eq}$ results, which establishes a fit error interval of $\pm$ ~~5.1~~ 5.0 K. This method only accounts for the fit error and does not take into account other potential sources of experimental error, as discussed below.

The precision of repeated measurements conducted at the same experimental conditions demonstrated a temperature dependence due to ClO or ClOOCl concentrations approaching their experimental limit of quantification (ClO limiting measurements

20 at colder temperatures and ClOOCl at warmer temperatures). To assess the significance of the lower precision at temperatures above 290 K and below 250 K, weighted least-squares third law fits were performed on sub-sampled data populations. An analysis of $K_{eq}$ results obtained between 250 – 301 K, 229 – 291 K, and 250 – 291 K resulted in $B$ parameters of ~~8531 K, 8534~~ 8527 K, 8529 K, and ~~8533~~ 8528 K, respectively, which deviate minimally from the parameter of ~~8533~~ 8528 K obtained from a fit of the entire temperature range. The extrapolated value of $K_{eq}$ at 200 K obtained from these sub-sampled datasets

25 varies by $< 1\%$, while at 180 K the spread of the maximal deviation in $K_{eq}$ between subsets is $< 2\%$. An estimate of error from temperature-dependent precision is $\pm$ 2 K about the $B$ parameter. The precision of repeated measurements conducted at the same temperature but varied flow rates and pressures did not statistically deviate from the precision from temperature-dependence alone.

Variation in the reference cross section of one component in a multicomponent fit may impact the quality of fit for the other

30 spectral components. It is the trend in the literature to not explicitly include uncertainties from the reference cross sections during assignation of error for $K_{eq}$; however, the choice of synthetic cross sections for ClO is considered further here. As discussed, the synthetic temperature-dependent ClO cross sections prepared by Marić and Burrows (1999) were employed for the determination of [ClO] in this study, and the ClO concentrations from fits using these synthetic cross sections differed from ClO concentrations determined using experimentally derived reference standards at most by 2.7%. To capture the uncertainty of this error, all ClO concentrations used to derive $K_{eq}$ were scaled by $\pm$ 2.7% and then fit by a weighted least-squares third law analysis, producing an estimated error in $B$ due to ClO cross section selection of $\pm$ 13 K.

The selection of the wavelength window used for the spectral fit also produced variations in derived concentrations, and
5  consequently $K_{eq}$, but the impact was not substantial. Ultimately, estimating our uncertainty on the $B$ parameter from all
known sources of potential error yielded comparable, but smaller, values than simply assigning the error interval such that it
fully encompassed 95% of the individual (unbinned) $K_{eq}$ results. Accordingly, we assign error intervals ($1\sigma$) to our $B$ parameter
of $\pm 25$ K. Systematic errors arising from experimental design and post-processing technique are estimated to contribute errors
that sum to a total smaller than this boundary. Our resulting $K_{eq}$ expression from the third law fit is shown in equation (3).

10  $$K_{eq} = 2.16 \times 10^{-27} e^{(8533 \pm 25 \text{ K}/T)(8528 \pm 25 \text{ K}/T)} \text{ cm}^3 \text{ molecule}^{-1} \tag{3}$$

Figure 4 provides a comparison of our results (purple circles) to equilibrium constants determined from other laboratory
studies. In this and subsequent figures, our data were binned in 5 K intervals, with each $K_{eq}$ point plotted at the average
temperature of the data collected within the binning interval. The presentation of binned data is for improved figure clarity
only; all data analyses were performed with the 87 independent experiments (Table 1). Notably in Figure 4, the $K_{eq}$ values
15  reported in this work are typically smaller than prior evaluations of $K_{eq}$ at warmer temperatures but match well with the colder
temperature observations of Hume et al. (2015) for those data points with overlap (228 – 250 K). Moreover, our third law fit
matches well with the results of Hume et al. (2015) when extrapolated to 200 K.

The ratio of $K_{eq}$ values from prior laboratory studies relative to $K_{eq}$ calculated from equation (3) is shown in Figure 45. The
$1\sigma$ ($B\pm 25$ K) and $2\sigma$ ($B\pm 50$ K) error bounds from this work are plotted as shaded gray tones. The $K_{eq}$ values from previous
20  laboratory studies were derived using either UV absorption spectroscopy of equilibrium mixtures of ClO and ClOOCl or by
determination of the individual forward and/or reverse kinetic rates of dimerization, reaction (R1). Experimental data from
these previous studies are shown as circles and triangles, respectively. As evident in Figure 45, there is much greater variation
in the determinations of $K_{eq}$ using kinetics methods.

The experiments of Cox and Hayman (1988) and Hume et al. (2015) were performed by UV analysis. The results of Hume
25  et al. (2015) lie almost entirely within our $1\sigma$ error interval. Though the individual results of Cox and Hayman exhibit significant
scatter and some measurements exceed the $2\sigma$ error reported here, an ordinary least-squares third law fit of their results using
the JPL-recommended $A$ parameter (Burkholder et al., 2015) remains within our $1\sigma$ error boundaries.

Nickolaisen et al. (1994) and Ferracci and Rowley (2010) used flash photolysis/UV absorption spectroscopy to determine
the kinetic rates of the individual reactions in order to determine $K_{eq}$. Though these two studies agree with each other in trend
30  and magnitude, they both exhibit significant departures from our results, possibly due to secondary reactions given the high
concentrations of ClO and $Cl_2O$ employed in those studies.

Bröske and Zabel (2006) investigated the kinetics of the ClOOCl dissociation reaction and estimated $K_{eq}$ values using
JPL 2002 kinetics (Sander et al., 2003) for the forward reaction (R1). A reanalysis of their results using JPL 2015 kinetics
(Burkholder et al., 2015) is plotted as binned averages in Figure 45 (orange triangles, $P < 30$ mbar; brown triangles, $P >$
30 mbar). A reanalysis of the high-pressure results of Bröske and Zabel (2006) also provides a third law fit ($K_{eq} = 2.16 \times$

$10^{-27} \mathrm{e}^{(8498\,\mathrm{K}/T)}$ cm$^3$ molecule$^{-1}$ that resides within our $2\sigma$ error limits. The discrepancy between the experiments of Bröske and Zabel (2006) conducted at higher pressures and lower pressures is discussed in depth in their work.

5     Horowitz et al. (1994) examined the loss rate of ClO while monitoring the kinetics and branching ratio of the ClO + ClO reaction and provide a single-point estimate of $K_{\mathrm{eq}}$ at 285 K that is ~~only 3% higher than~~ within $1\sigma$ of the value determined at that temperature in this work. However, the $K_{\mathrm{eq}}$ values of Boakes et al. (2005) using flash photolysis/UV absorption spectroscopy, Ellermann et al. (1995) using pulsed radiolysis/UV absorption spectroscopy, and Plenge et al. (2005) via mass spectrometric determination of the ClO-OCl bond strength, all lie outside the $2\sigma$ error limits from this work.

10     Figure ~~5~~ 6 provides a comparison between observational determinations of $K_{\mathrm{eq}}$ in the atmosphere and an extrapolation of $K_{\mathrm{eq}}$ from this work to 190 K. The determination of $K_{\mathrm{eq}}$ by Avallone and Toohey (2001), an analysis of AASE I and AASE II data in which mixing ratios of ClOOCl were inferred from total Cl$_y$ mass conservation rather than directly measured, agree within error with the results of this work. Similarly, a determination of $K_{\mathrm{eq}}$ by Santee et al. (2010), informed by ClO mixing ratios retrieved via Aura MLS satellite data and ClOOCl mixing ratios calculated from stratospheric modeling, lies in substantial agreement

15 with the $K_{\mathrm{eq}}$ expression derived here. ~~The~~ All observed ratios of [ClOOCl] / [ClO]$^2$ in the Arctic stratosphere for the nighttime ER-2 flight of 3 Feb 2000 during the SOLVE/THESEO campaign ~~(black crosses)~~ (Stimpfle et al., 2004) also agree within ~~measurement uncertainties (Stimpfle et al., 2004)~~ the combined $2\sigma$ measurement uncertainties (SOLVE/THESEO measurement uncertainties not plotted for clarity). The $K_{\mathrm{eq}}$ expression from von Hobe et al. (2005), which was based on observations in Arctic winter 2003, deviates substantially from $K_{\mathrm{eq}}$ determined in this work; however, von Hobe et al. (2007) postulate that

20 those previous observations of ClO and ClOOCl may not have been in equilibrium and that the ClOOCl measurements may have been biased low.

    A thermodynamic representation of parameters $A$ and $B$ [equation (2)] can be obtained from a manipulation of the van't Hoff equation. The prefactor $A$ encodes the standard entropy of reaction change per equation (4), in which the superscript indicates a standard state of one bar, $R'$ is the gas constant (83.145 cm$^3$ bar mol$^{-1}$ K$^{-1}$), $N_{\mathrm{A}}$ is Avogadro's constant (6.0221 $\times$

25 $10^{23}$ molecules mol$^{-1}$), $R$ is the gas constant in energy units (8.3145 J mol$^{-1}$ K$^{-1}$), $e$ is Euler's number, and $T$ is system temperature.

$$\Delta S^{\circ}(298\ \mathrm{K}) = R\ln\left(\frac{N_{\mathrm{A}}A}{eR'T}\right) \tag{4}$$

    The exponential argument $B$ relates the change in standard enthalpy of reaction as shown in equation (5), with $R$ and $T$ as defined above.

30   $$\Delta H^{\circ}(298\ \mathrm{K}) = -R(T+B) \tag{5}$$

    Evaluating equation (5) with our derived value of $B$ = ~~8533~~ 8528 K results in a $\Delta H^{\circ}(298\ \mathrm{K})$ of -73.4 $\pm$ 0.6 kJ mol$^{-1}$ for reaction (R1). The uncertainty estimate on this value was obtained by combining the previously determined uncertainty on our $B$ parameter ($\pm$ 25 K) with estimated uncertainties in the reference cross sections for ClOOCl [$\pm$ 17% variation near the peak

cross section at 248 nm, as reported by Lien et al. (2009), Papanastasiou et al. (2009), and Wilmouth et al. (2009)] and for ClO
[± 3% variation in the peak of the absorption continuum at 264 nm between Sander and Friedl (1988), Simon et al. (1990),

5  and Trolier et al. (1990)] to produce a possible range in $B$ of ~~8464 K to 8602~~ 8453 K to 8604 K, as determined from scaled,
third law ~~weighted~~ least-squares fits.

Combining our $\Delta H^{\circ}(298\text{ K})$ value for reaction (R1) with the JPL-recommended $\Delta H_f^{\circ}(298\text{ K})$ for ClO of $101.681 \pm 0.040$
kJ mol$^{-1}$ (Burkholder et al., 2015) yields a $\Delta H_f^{\circ}(298\text{ K})$ for ClOOCl of ~~129.9~~ 130.0 $\pm$ 0.6 kJ mol$^{-1}$. This result is in excellent
agreement with the JPL-recommended value of $130.1 \pm 1$ kJ mol$^{-1}$.

10  A ~~weighted~~ least-squares second law fit of $K_{\text{eq}}$, in which both $A$ and $B$ are free parameters, yields a determination of $K_{\text{eq}}$
as shown in equation (6).

$$K_{\text{eq}} = \left( \text{\textcolor{red}{2.06}} 2.14 \pm \text{\textcolor{red}{1.27}} 1.14 \right) \times 10^{-27} e^{(\text{\textcolor{red}{8546 \pm 123\,K/T}})(8530 \pm 123\,K/T)} \text{ cm}^3 \text{ molecule}^{-1} \qquad (6)$$

An application of equation (4) to the second law prefactor of ~~$2.06 \times 10^{-27}$~~ $2.14 \times 10^{-27}$ cm$^3$ molecule$^{-1}$ produces $\Delta S^{\circ}(298\text{ K})$
= ~~$-148.1 \pm 4.0$~~ $-147.8 \, (^{+3.6}_{-6.3})$ J mol$^{-1}$ K$^{-1}$ for reaction (R1), which agrees with the JPL-recommended value of -147.0 J mol$^{-1}$

15  K$^{-1}$ [calculated from the $S$ values for ClO and ClOOCl in Table 6-2 of Burkholder et al. (2015)]. The value of $\Delta H^{\circ}(298\text{ K})$
of ~~-73.5~~ -73.4 $\pm$ 1.0 kJ mol$^{-1}$ for reaction (R1) from the second law analysis is in excellent agreement with our results from
the third law analysis.

Notably, the equilibrium constant results obtained in this work agree in trend and magnitude with the recently reported $K_{\text{eq}}$
values of Hume et al. (2015). This excellent correspondence is illustrated in Figure ~~6~~ 7, in which a ~~weighted~~ least-squares third

20  law fit (with each study weighted equally) is presented for a combined data set containing the results of this work and the
work of Hume et al. (2015) in ratio to the current JPL recommendation (Burkholder et al., 2015). The combined works span a
temperature range of 206 – 301 K, and the resulting $K_{\text{eq}}$ is 2.16 ~~$\times 10^{-27} e^{(8535\,K/T)}$~~ $\times 10^{-27} e^{(8533\,K/T)}$ cm$^3$ molecule$^{-1}$. This
expression deviates from the JPL-recommended $K_{\text{eq}}$ value at 200 K by ~~about 1~~ 2%. For illustrative purposes, the uncertainty
bounds calculated from this work and the bounds recommended by the current JPL evaluation (Burkholder et al., 2015) are

25  also plotted. The JPL uncertainty, which was scaled to include the warm temperature results of Cox and Hayman (1988) and
Nickolaisen et al. (1994), greatly exceeds the scatter of the individual $K_{\text{eq}}$ values from the combined dataset of this work and
Hume et al. (2015). Our results suggest that the uncertainties in the current JPL recommendation for $K_{\text{eq}}$ can be significantly
reduced.

## 4  Conclusions

The thermal equilibrium governing the association of ClO and dissociation of ClOOCl was investigated in a custom-built
discharge-flow reactor by UV spectroscopy between the temperatures of 228 – 301 K. The selected temperature range allowed
us to bridge the warmer temperature regime where nearly all previous laboratory studies of $K_{\text{eq}}$ have been performed and the

5  recent colder temperature work of Hume et al. (2015). A third law fit of our $K_{\text{eq}}$ results deviates from some prior laboratory

studies but demonstrates excellent agreement with the work of Hume et al. (2015) and with the currently recommended parameters in the JPL compendium (Burkholder et al., 2015). The agreement between our third law and second law analyses lends further confidence to the results reported herein. Our calculated enthalpy of formation for ClOOCl from the slope of the van't Hoff plot is in excellent agreement with the recommended value (Burkholder et al., 2015).

5    The current JPL-recommended error bounds for the ClO-ClOOCl equilibrium constant are large (Burkholder et al., 2015), exceeding 50% at 200 K. The excellent correspondence between the $K_{eq}$ results from this work and Hume et al. (2015) lends confidence to the established parameterization of the JPL data evaluation (Burkholder et al., 2015), suggesting that prescribed error intervals for this reaction can be reduced.

# References

15    Avallone, L. M. and Toohey, D. W.: Tests of halogen photochemistry using in situ measurements of ClO and BrO in the lower polar strato-sphere, J. Geophys. Res.-Atmos., 106, 10 411 – 10 421, https://doi.org/10.1029/2000JD900831, 2001.

Boakes, G., Hindy Mok, W. H., and Rowley, D. M.: Kinetic studies of the ClO + ClO association reaction as a function of temperature and pressure, Phys. Chem. Chem. Phys., 7, 4102 – 4113, https://doi.org/10.1039/B510308H, 2005.

Bröske, R. and Zabel, F.: Thermal decomposition of ClOOCl, J. Phys. Chem. A, 110, 3280 – 3288, https://doi.org/10.1021/jp0550053, 2006.

20    Burkholder, J. B., Sander, S. P., Abbatt, J. P. D., Barker, J. R., Huie, R. E., Kolb, C. E., Kurylo, M. J., Orkin, V. L., Wilmouth, D. M., and Wine, P. H.: Chemical kinetics and photochemical data for use in atmospheric studies, evaluation no. 18, JPL Publication 15-10, Jet Propulsion Laboratory, Pasadena, 2015.

Canty, T. P., Salawitch, R. J., and Wilmouth, D. M.: The kinetics of the ClOOCl catalytic cycle, J. Geophys. Res.-Atmos., 121, 13 768 – 13 783, https://doi.org/10.1002/2016JD025710, 2016.

25    Cox, R. A. and Hayman, G. D.: The stability and photochemistry of dimers of the ClO radical and implications for Antarctic ozone depletion, Nature, 332, 796 – 800, https://doi.org/10.1038/332796a0, 1988.

Ellermann, T., Johnsson, K., Lund, A., and Pagsberg, P.: Kinetics and equilibrium constant of the reversible reaction ClO + ClO + M $\leftrightharpoons$ Cl$_2$O$_2$ + M at 295 K, Acta Chem. Scand., 49, 28 – 35, https://doi.org/10.3891/acta.chem.scand.49-0028, 1995.

Ferracci, V. and Rowley, D. M.: Kinetic and thermochemical studies of the ClO + ClO + M $\leftrightharpoons$ Cl$_2$O$_2$ + M reaction, Phys. Chem. Chem.
30    Phys., 12, 11 596 – 11 608, https://doi.org/10.1039/c0cp00308e, 2010.

Horowitz, A., Crowley, J. N., and Moortgat, G. K.: Temperature dependence of the product branching ratios of the ClO self-reaction in oxygen, J. Phys. Chem., 98, 11 924 – 11 930, https://doi.org/10.1021/j100097a019, 1994.

Hume, K. L., Bayes, K. D., and Sander, S. P.: Equilibrium constant for the reaction ClO + ClO ↔ ClOOCl between 250 and 206 K, J. Phys. Chem. A, 119, 4473 – 4481, https://doi.org/10.1021/jp510100n, 2015.

35    Kromminga, H., Orphal, J., Spietz, P., Voigt, S., and Burrows, J. P.: New measurements of OClO absorption cross-sections in the 325–435 nm region and their temperature dependence between 213 and 293 K, J. Photoch. Photobio. A, 157, 149 – 160, https://doi.org/10.1016/S1010-6030(03)00071-6, 2003.

Lien, C.-Y., Lin, W.-Y., Chen, H.-Y., Huang, W.-T., Jin, B., Chen, I.-C., and Lin, J. J.: Photodissociation cross sections of ClOOCl at 248.4 and 266 nm, J. Chem. Phys., 131, 174 301, https://doi.org/10.1063/1.3257682, 2009.

Marić, D. and Burrows, J. P.: Analysis of the UV absorption spectrum of ClO: a comparative study of four methods for spectral computations,
5    J. Quant. Spectrosc. RA, 62, 345 – 369, https://doi.org/10.1016/S0022-4073(98)00108-3, 1999.

Marić, D., Burrows, J. P., Meller, R., and Moortgat, G. K.: A study of the UV-visible absorption spectrum of molecular chlorine, J. Photoch. Photobio. A, 70, 205 – 214, https://doi.org/10.1016/1010-6030(93)85045-A, 1993.

Molina, L. T. and Molina, M. J.: Absolute absorption cross sections of ozone in the 185- to 350-nm wavelength range, J. Geophys. Res.-Atmos., 91, 14 501 – 14 508, https://doi.org/10.1029/JD091iD13p14501, 1986.

10    Molina, L. T. and Molina, M. J.: Production of chlorine oxide (Cl$_2$O$_2$) from the self-reaction of the chlorine oxide (ClO) radical, J. Phys. Chem., 91, 433 – 436, https://doi.org/10.1021/j100286a035, 1987.

Newville, M., Stensitzki, T., Allen, D. B., Rawlik, M., Ingargiola, A., and Nelson, A.: LMFIT: non-linear least-square minimization and curve-fitting for Python, Astrophysics Source Code Library, 2016.

Nickolaisen, S. L., Friedl, R. R., and Sander, S. P.: Kinetics and mechanism of the chlorine oxide ClO + ClO reaction: pressure and temperature dependences of the bimolecular and termolecular channels and thermal decomposition of chlorine peroxide, J. Phys. Chem., 98, 155 – 169, https://doi.org/10.1021/j100052a027, 1994.

Papanastasiou, D. K., Papadimitriou, V. C., Fahey, D. W., and Burkholder, J. B.: UV absorption spectrum of the ClO dimer ($Cl_2O_2$) between 200 and 420 nm, J. Phys. Chem. A, 113, 13 711 – 13 726, https://doi.org/10.1021/jp9065345, 2009.

Plenge, J., Kühl, S., Vogel, B., Müller, R., Stroh, F., von Hobe, M., Flesch, R., and Rühl, E.: Bond strength of chlorine peroxide, J. Phys. Chem. A, 109, 6730 – 6734, https://doi.org/10.1021/jp044142h, 2005.

Sander, S. P. and Friedl, R. R.: Kinetics and product studies of the BrO + ClO reaction: Implications for Antarctic chemistry, Geophys. Res. Lett., 15, 887 – 890, https://doi.org/10.1029/GL015i008p00887, 1988.

Sander, S. P., Friedl, R. R., Ravishankara, A. R., Golden, D. M., Kolb, C. E., Kurylo, M. J., Huie, R. E., Orkin, V. L., Molina, M. J., Moortgat, G. K., and Finlayson-Pitts, B. J.: Chemical kinetics and photochemical data for use in atmospheric studies, evaluation no. 14, JPL Publication 02-25, Jet Propulsion Laboratory, Pasadena, 2003.

Sander, S. P., Friedl, R. R., Abbatt, J. P. D., Barker, J. R., Burkholder, J. B., Golden, D. M., Kolb, C. E., Kurylo, M. J., Moortgat, G. K., Wine, P. H., Huie, R. E., and Orkin, V. L.: Chemical kinetics and photochemical data for use in atmospheric studies, evaluation no. 17, JPL Publication 10-6, Jet Propulsion Laboratory, Pasadena, 2011.

Santee, M. L., Sander, S. P., Livesey, N. J., and Froidevaux, L.: Constraining the chlorine monoxide (ClO)/chlorine peroxide (ClOOCl) equilibrium constant from Aura Microwave Limb Sounder measurements of nighttime ClO, Proc. Natl. Acad. Sci. U. S. A., 107, 6588i – 6593, https://doi.org/10.1073/pnas.0912659107, 2010.

Simon, F. G., Schneider, W., Moortgat, G. K., and Burrows, J. P.: A study of the ClO absorption cross-section between 240 and 310 nm and the kinetics of the self-reaction at 300 K, J. Photoch. Photobio. A, 55, 1 – 23, https://doi.org/10.1016/1010-6030(90)80014-O, 1990.

Stimpfle, R. M., Wilmouth, D. M., Salawitch, R. J., and Anderson, J. G.: First measurements of ClOOCl in the stratosphere: the coupling of ClOOCl and ClO in the Arctic polar vortex, J. Geophys. Res.-Atmos., 109, D03 301, https://doi.org/10.1029/2003JD003811, 2004.

Trolier, M., Mauldin, R. L., and Ravishankara, A. R.: Rate coefficient for the termolecular channel of the self-reaction of chlorine monoxide, J. Phys. Chem., 94, 4896 – 4907, https://doi.org/10.1021/j100375a027, 1990.

von Hobe, M., Grooß, J.-U., Müller, R., Hrechanyy, S., Winkler, U., and Stroh, F.: A re-evaluation of the ClO/$Cl_2O_2$ equilibrium constant based on stratospheric in-situ observations, Atmos. Chem. Phys., 5, 693 – 702, https://doi.org/10.5194/acp-5-693-2005, 2005.

von Hobe, M., Salawitch, R. J., Canty, T., Keller-Rudek, H., Moortgat, G. K., Grooß, J.-U., Müller, R., and Stroh, F.: Understanding the kinetics of the ClO dimer cycle, Atmos. Chem. Phys., 7, 3055 – 3069, https://doi.org/10.5194/acp-7-3055-2007, 2007.

Wilmouth, D. M., Hanisco, T. F., Stimpfle, R. M., and Anderson, J. G.: Chlorine-catalyzed ozone destruction: Cl atom production from ClOOCl photolysis, J. Phys. Chem. A, 113, 14 099 – 14 108, https://doi.org/10.1021/jp9053204, 2009.

Wilmouth, D. M., Salawitch, R. J., and Canty, T. P.: Stratospheric Ozone Depletion and Recovery, in: Green chemistry: an inclusive approach, edited by Torok, B. and Dransfield, T., chap. 3.3, pp. 177 – 209, Elsevier, 2018.

WMO: Scientific Assessment of Ozone Depletion: 2014, World Meteorological Organization, Global Ozone Research and Monitoring Project - Report No. 55, WMO, Geneva, 2014.

Wohltmann, I., Lehmann, R., and Rex, M.: A quantitative analysis of the reactions involved in stratospheric ozone depletion in the polar vortex core, Atmos. Chem. Phys., 17, 10 535, https://doi.org/10.5194/acp-17-10535-2017, 2017.
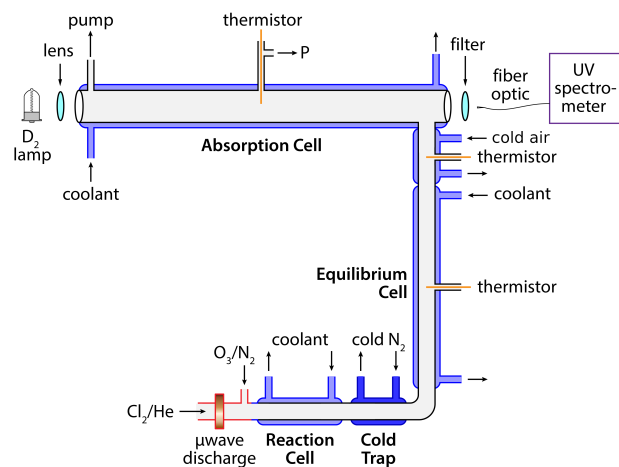
**Figure 1.** Schematic of the discharge-flow absorbance experiment. Dilute chlorine gas in helium flows through a microwave discharge to form Cl radicals. Dilute ozone in nitrogen is then injected to produce ClO radicals. Self-reaction of ClO occurs in the cold reaction cell to form ClOOCl. When utilized, the cold trap provides for halogen oxide purification. ClO/ClOOCl equilibrium is established in the equilibrium cell, which is held at the same temperature as the absorption cell. The gas mixture is then characterized via UV spectroscopy in the absorption cell using software developed in-house.
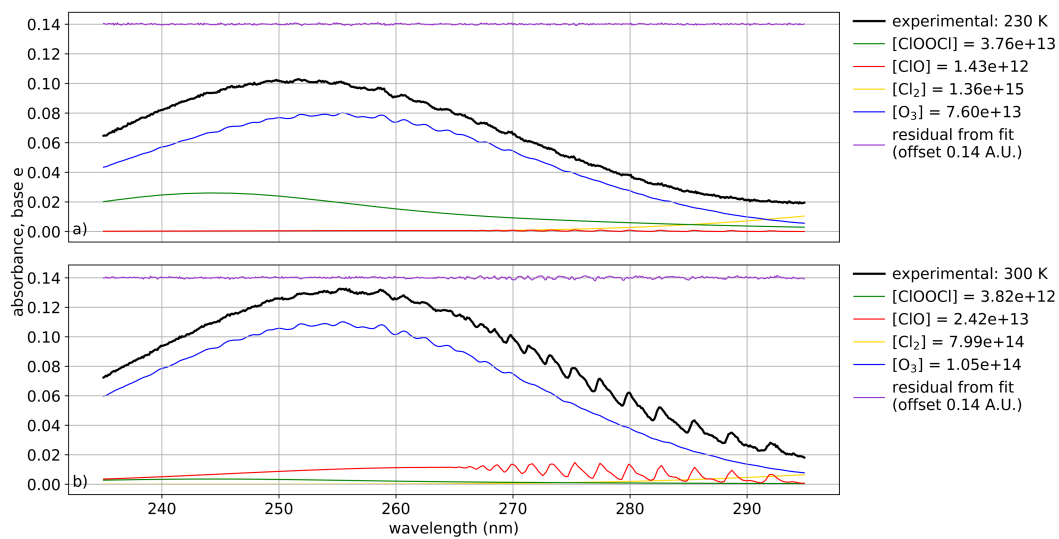
**Figure 2.** Deconvolution of experimental absorbance spectra to component contributions. (a) Experimental spectrum obtained at 230 K. (b) Experimental spectrum obtained at 300 K. In each panel, the raw absorbance spectrum appears as a black line, and the fitted components and residual from the fit are shown. Fitted concentrations (molecules cm$^{-3}$) are given for various component gases in the legend. The residual is offset by 0.14 A.U. for clarity. OClO and $Cl_2O_3$ contributions are small, especially at low temperatures, and are omitted from the figure.
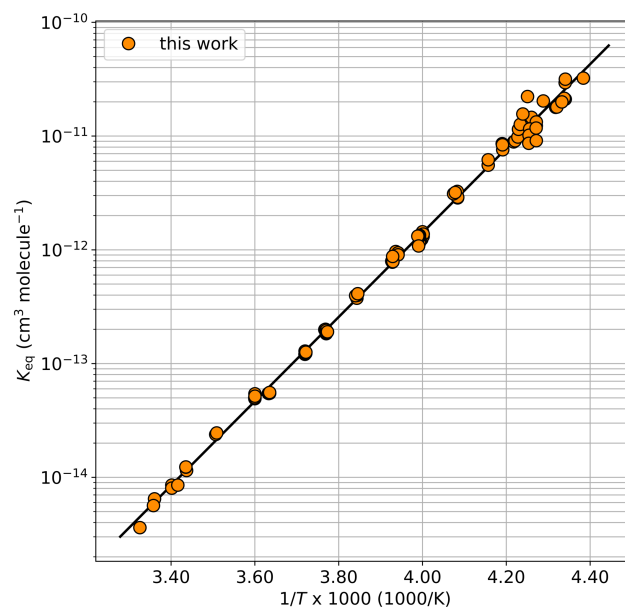
**Figure 3.** Experimental $K_{eq}$ values as a function of $1000/T$. The black trace is a third law fit of the orange circles, $K_{eq} = 2.16 \times 10^{-27} e^{(8528 \text{ K}/T)}$ cm$^3$ molecule$^{-1}$. Individual values are enumerated in Table 1.
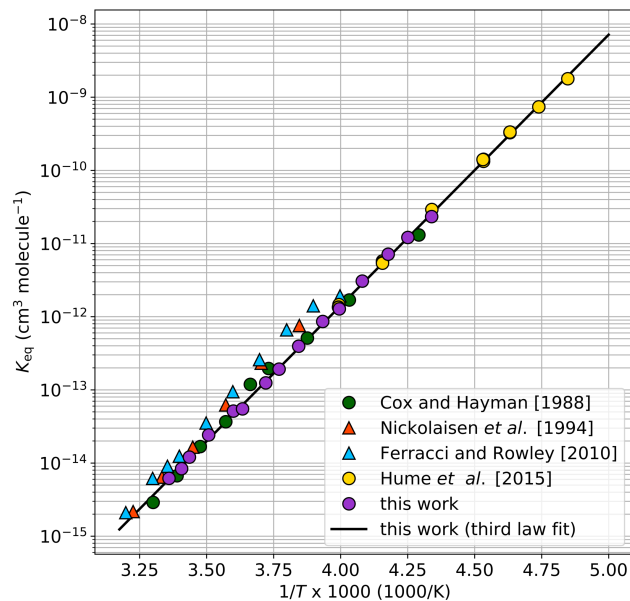
**Figure 4.** $K_{eq}$ values as a function of 1000/T. Data from this work are plotted as purple circles; for figure clarity, multiple samples (Table 1) are binned and averaged in 5 K intervals~~as shown in Table 1.~~. The black ~~line~~ trace is ~~a~~ the third law fit ~~of the purple circles~~ as determined in Figure 3, $K_{eq} = $ ~~$2.16 \times 10^{-27} e^{(8533 \, \text{K}/T)}$~~ $2.16 \times 10^{-27} e^{(8528 \, \text{K}/T)}$ cm$^3$ molecule$^{-1}$. The colored markers are $K_{eq}$ values from prior laboratory studies as reported in the literature.
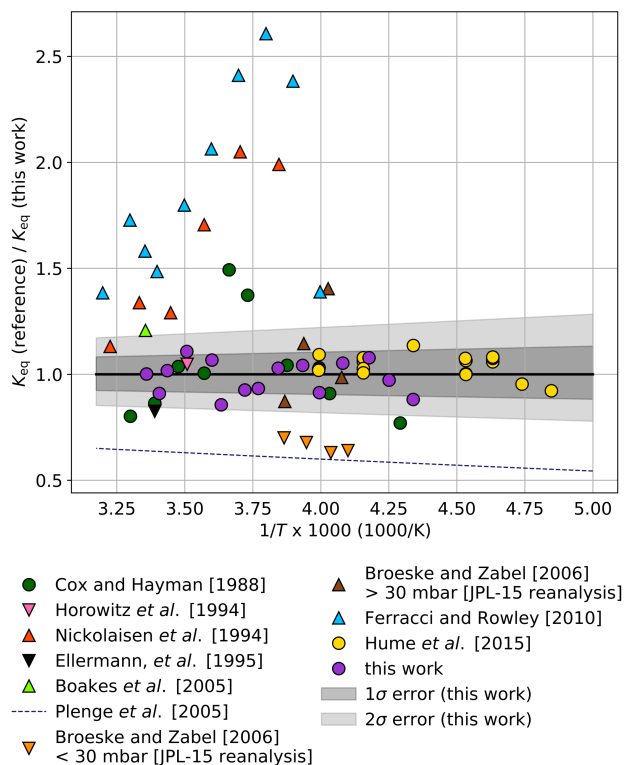
**Figure 5.** Ratio of $K_{eq}$ values from prior laboratory studies to $K_{eq}$ determined in this work ($K_{eq}$ = ~~$2.16 \times 10^{-27} e^{(8533\,\mathrm{K}/T)}$~~ $2.16 \times 10^{-27} e^{(8528\,\mathrm{K}/T)}$ cm$^3$ molecule$^{-1}$) as a function of $1000/T$. Circles indicate studies in which $K_{eq}$ was measured with UV spectroscopy of equilibrium mixtures, while triangles indicate works in which $K_{eq}$ was determined from individual reaction kinetic rates. Dark gray shading encompasses the total estimated $1\sigma$ error from this study and light shading encompasses the $2\sigma$ error.
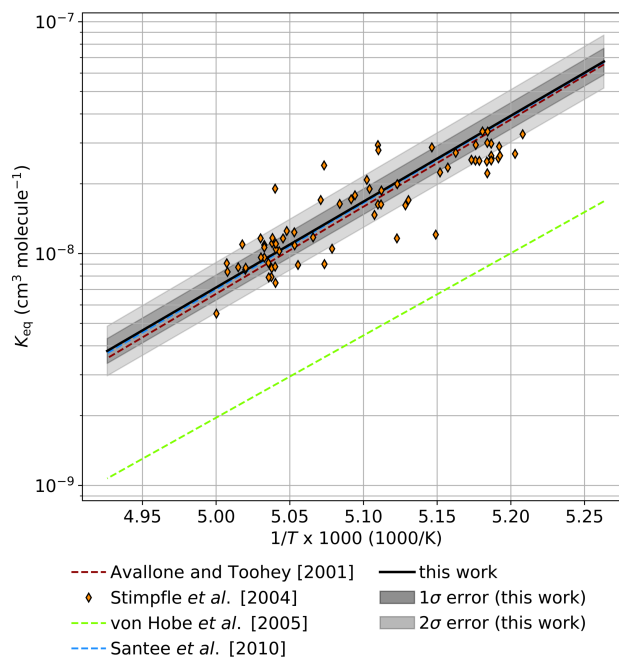
**Figure 6.** Comparison of extrapolated $K_{eq}$ values from ~~the third law fit in~~ this work ($K_{eq} = 2.16 \times 10^{-27} e^{(8528\,K/T)}$ $cm^3$ $molecule^{-1}$) to atmospheric observations. $K_{eq}$ (solid black) and error boundaries (gray shaded regions) determined in this study are extrapolated to the temperature range of 190 – 203 K. Expressions for $K_{eq}$ derived from previous atmospheric measurements are presented as dashed lines. Observations of [ClOOCl] / [ClO]$^2$ from the nighttime ER-2 flight on 3 Feb 2000 in the SOLVE/THESEO mission out of Kiruna, Sweden are indicated as ~~black crosses~~orange diamonds.

**Figure 7.** Ratio of a weighted third law fit of $K_{eq}$ (black dashed line) determined from a combination of this work (circles) and Hume et al. (2015) (triangles) to the JPL compendium recommended value (Burkholder et al., 2015). Error intervals as reported in this work (darker blue = $1\sigma$, lighter blue = $2\sigma$) and as recommended by JPL-2015 (red cross hatch).

**Table 1.** Experimental conditions and $K_{eq}$ values

| $T^a$ (K) | $P$ (mbar) | $K_{eq}$ (cm$^3$ molecule$^{-1}$) | $T^a$ (K) | $P$ (mbar) | $K_{eq}$ (cm$^3$ molecule$^{-1}$) | $S^b_K$ |
|---|---|---|---|---|---|---|
| 300.70 | 100 | $3.61 \times 10^{-15}$ | 265.07 | 200 | $1.89 \times 10^{-13}$ | 240 |
| 297.80 | 100 | $5.65 \times 10^{-15}$ | 265.02 | 200 | $1.90 \times 10^{-13}$ | 240 |
| 297.57 | 100 | $6.48 \times 10^{-15}$ | 260.38 | 233 | $3.96 \times 10^{-13}$ | 238 |
| 294.98 | 100 | $8.55 \times 10^{-15}$ | 260.18 | 233 | $3.75 \times 10^{-13}$ | 238 |
| 294.97 | 100 | $8.04 \times 10^{-15}$ | 260.15 | 233 | $3.98 \times 10^{-13}$ | 238 |
| 292.74 | 100 | $8.54 \times 10^{-15}$ | 260.04 | 233 | $4.12 \times 10^{-13}$ | 237 |
| 291.10 | 133 | $1.23 \times 10^{-14}$ | 254.66 | 233 | $7.95 \times 10^{-13}$ | 230 |
| 291.09 | 133 | $1.23 \times 10^{-14}$ | 254.57 | 233 | $7.79 \times 10^{-13}$ | 230 |
| 291.96 | 133 | $1.15 \times 10^{-14}$ | 254.53 | 233 | $8.75 \times 10^{-13}$ | 230 |
| 285.18 | 133 | $2.38 \times 10^{-14}$ | 254.49 | 233 | $7.87 \times 10^{-13}$ | 230 |
| 285.00 | 133 | $2.46 \times 10^{-14}$ | 254.05 | 233 | $9.66 \times 10^{-13}$ | 233 |
| 277.79 | 167 | $5.01 \times 10^{-14}$ | 253.70 | 233 | $9.04 \times 10^{-13}$ | 233 |
| 277.79 | 167 | $4.92 \times 10^{-14}$ | 253.70 | 233 | $9.43 \times 10^{-13}$ | 233 |
| 277.77 | 167 | $5.42 \times 10^{-14}$ | 250.71 | 267 | $1.32 \times 10^{-12}$ | 233 |
| 277.76 | 167 | $5.17 \times 10^{-14}$ | 250.58 | 267 | $1.08 \times 10^{-12}$ | 233 |
| 275.32 | 167 | $5.48 \times 10^{-14}$ | 250.56 | 267 | $1.32 \times 10^{-12}$ | 234 |
| 275.25 | 167 | $5.46 \times 10^{-14}$ | 250.51 | 267 | $1.29 \times 10^{-12}$ | 234 |
| 275.09 | 167 | $5.48 \times 10^{-14}$ | 250.45 | 267 | $1.16 \times 10^{-12}$ | |
| 275.08 | 167 | $5.58 \times 10^{-14}$ | 250.45 | 267 | $1.34 \times 10^{-12}$ | |
| 268.85 | 200 | $1.21 \times 10^{-13}$ | 250.36 | 267 | $1.22 \times 10^{-12}$ | 234 |
| 268.83 | 200 | $1.29 \times 10^{-13}$ | 250.11 | 267 | $1.24 \times 10^{-12}$ | 233 |
| 268.71 | 200 | $1.23 \times 10^{-13}$ | 250.00 | 267 | $1.44 \times 10^{-12}$ | 23 |
| 268.69 | 200 | $1.26 \times 10^{-13}$ | 249.90 | 267 | $1.31 \times 10^{-12}$ | 23 |
| 265.47 | 200 | $1.99 \times 10^{-13}$ | 249.89 | 267 | $1.37 \times 10^{-12}$ | 230 |
| 265.35 | 200 | $2.00 \times 10^{-13}$ | 245.44 | 267 | $3.11 \times 10^{-12}$ | 230 |
| 265.23 | 200 | $1.83 \times 10^{-13}$ | 245.21 | 267 | $3.19 \times 10^{-12}$ | 230 |
| 265.21 | 200 | $1.86 \times 10^{-13}$ | 244.92 | 267 | $3.27 \times 10^{-12}$ | 230 |
| 265.21 | 200 | $1.95 \times 10^{-13}$ | 244.87 | 267 | $2.86 \times 10^{-12}$ | 230 |
| 265.20 | 200 | $1.96 \times 10^{-13}$ | 244.85 | 267 | $2.90 \times 10^{-12}$ | 229 |

[a] Temperature reported to five significant figures for purposes of fitting.